

pubs.acs.org/JCTC Article

EE-ONIOM-CT Method to Efficiently Account for the Missing Interactions in ONIOM: Energies and Analytic Gradients

Vikrant Tripathy* and Krishnan Raghavachari*



Cite This: J. Chem. Theory Comput. 2023, 19, 5791-5805



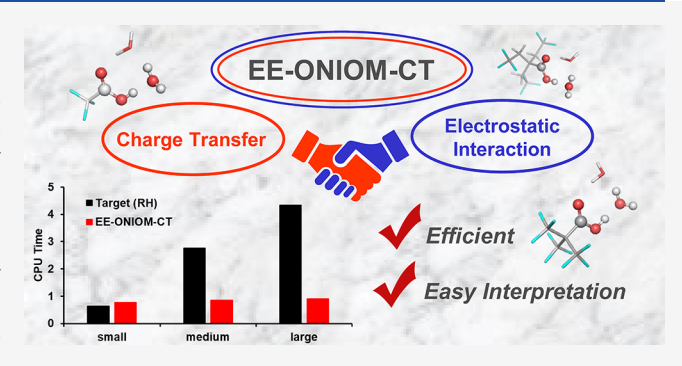
ACCESS I

III Metrics & More

Article Recommendations

s Supporting Information

ABSTRACT: Hybrid methods such as ONIOM (QM:QM) are widely used for the study of local processes in large systems. However, the intrinsic need for system partitioning often leads to a less-than-desirable performance for some important chemical processes. This is due to the missing interactions in the chemically important model region (i.e., active site) of the high-level theory. The missing interactions can be categorized into two classes, viz. charge transfer (i.e., charge redistribution) and long-range electrostatic interactions. Our group presented two entirely different methods to treat these deficiencies individually. ONIOM-CT and ONIOM-EE methods have been demonstrated to improve the performance of ONIOM by incorporating charge



transfer and missing electrostatic interactions, respectively. In general, the inclusion of the missing interactions separately in two different calculations may not be sufficient to reach a high accuracy. Thus, it is highly desirable to develop a method to correct both deficiencies simultaneously. In this work, we aim to connect the methods ONIOM-CT and ONIOM-EE for a more comprehensive treatment. A "stepwise" model was found to be necessary for a robust performance. This model employs a stepwise procedure by first satisfying the ONIOM-CT condition for charge balance before accounting for the electrostatic interactions from the rest of the system perturbatively. This has the advantage of easy interpretation due to the clear separation of the two effects. We demonstrate the performance of our method using embedding charges determined from a Mulliken population analysis. An efficient analytic gradient expression for this method is derived and implemented by requiring three sets of z-vector self-consistent equations. The performance of our method is assessed against full system calculations in high-level theory for a set of three proton transfer reactions representing different degrees of electrostatic embedding.

1. INTRODUCTION

The computational cost of the in silico simulation of chemical reactions using electronic structure methods grows rapidly with system size, limiting the applicability of highly accurate methods to a modest number of atoms. This bottleneck may be overcome by realizing the local nature of most chemical processes. Hybrid methods take advantage of this aspect of chemical reactions by dividing molecules into different regions. Warshel and Levitt introduced QM/MM to study enzymic reactions where QM (charge distribution and bond cleavage in substrate) and MM (steric and electrostatic interactions between substrate and enzyme) complement each other. The general energy expression of QM/MM is given in eq 1. QM and MM energies are added, along with an interaction term. Thus, it is often referred to as an additive scheme.

$$E_{\text{QM/MM}} = E_{\text{QM}} + E_{\text{MM}} + E_{\text{QM-MM}}^{\text{Interaction}} \tag{1}$$

The interaction term, in eq 1, can be fairly convoluted and dependent on the choice of combination of methods and systems.^{3–5} Maseras and Morokuma suggested an alternative scheme called IMOMM (integrated molecular orbital+molec-

ular mechanics), avoiding any interaction term. This is often termed an extrapolation (or embedding) scheme. The IMOMM scheme, despite the ease of application, needs force field parameters for the QM region, which may not be available in many cases. A variant of this, called IMOMO, involving only QM methods, was proposed by Morokuma et al., which is more broadly applicable. Both of these methods were subsequently combined and extended to *n*-layers, which was called ONIOM (our own *N*-Layer integrated molecular orbital molecular mechanics). The flexibility in choice of number of layers and combination of methods enables a diverse set of applications. The development and application of this popular method is summarized in a recent review. The energy expression for the two-layer ONIOM is given in eq 2.

Received: May 12, 2023 Published: August 15, 2023





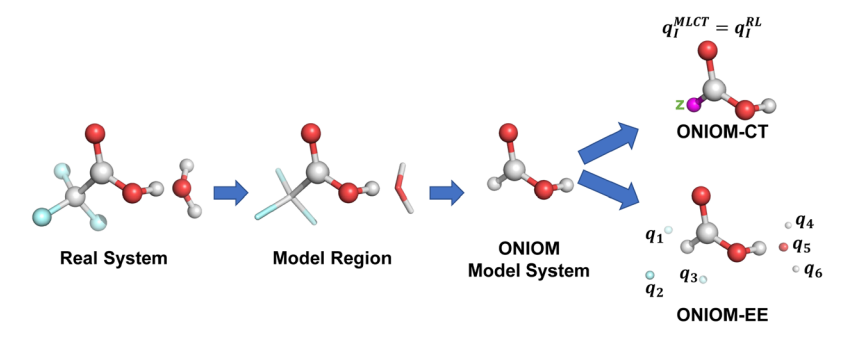


Figure 1. Workflow of the model system preparation for ONIOM-CT and ONIOM-EE methods. First the "Model region" is identified using chemical intuition. Model system is represented by ball and stick. ONIOM model system is prepared by placing a link atom to cap the dangling bond. ONIOM-CT corrects the charge transfer issues by placing a charge on the link atom nucleus (z). ONIOM-EE (point charge embedding) embeds the model system in external point charges placed at the position of atoms of rest of the system.

$$E_{\text{ONIOM}} = E_{\text{RL}} + E_{\text{MH}} - E_{\text{ML}} \tag{2}$$

Following standard notation, "high (H)" and "low (L)" represent the two different methods in hybrid calculations with higher and lower accuracy, respectively, and "model (M)" and "real (R)" regions represent the active region and the full system, respectively. Thus, the target energy is $E_{\rm RH}$ and the ONIOM error (S-value) is given by

$$Err_{ONIOM} = E_{ONIOM} - E_{RH}$$
 (3)

The aim of the two-layer ONIOM method is to approximate the computationally expensive RH calculation using three computationally inexpensive calculations (RL, ML, and MH). Typically, ONIOM is applied in chemical applications such as reaction energies, excitation energies, or relative energies where the difference in energy between two states removes systematic error. In addition, the simple form of the energy leads to the efficient calculation of properties and geometry optimizations. Vreven and Morokuma have summarized these applications in their review. ¹⁰

The necessity to split systems into multiple regions has the potential to introduce errors in hybrid methods, such as ONIOM. This is due to the missing interactions in the chemically important model region calculations. These interactions can be broadly classified into charge transfer and electrostatic interaction. The charge transfer (or charge imbalance) issues originate from the boundary passing through a covalent bond, and the electrostatic interactions are from the missing long-range effects from the rest of the system on the model region. In standard QM/MM and ONIOM, the resulting dangling bond due to the boundary passing through a covalent bond is capped using a hydrogen link atom. Standard QM/MM and ONIOM include polarization by fixed charges and low-level (RL) calculations, respectively.

Improvements to these oversimplified treatment of missing interactions have been achieved in QM/MM. Field¹¹ implemented the fluctuating charge model¹² based on electronegativity equalization method¹³ to condensed-phase simulations in QM/MM. Gao presented a molecular orbital-derived potential (MODEL) for QM/MM simulations.¹⁴ Several improved treatments^{15–17} of the boundary region in QM/MM have also been made, most notably GHO¹⁸ (generalized hybrid orbital), which, together with MODEL,¹⁴ constitutes the X-POL method.¹⁹ Variational formulation and implementation of analytic derivatives of the method enable efficient MD simulations.²⁰ The DSCF (double self-consistent

field) form has some similarity with fragmentation methods such as FMO^{21} and EE-MIM.

The analogous methods for ONIOM (QM:QM) have not yet been fully developed. Two different methods were proposed by our group to account for the missing interactions separately, viz., ONIOM-CT^{23,24} (ONIOM with Charge Transfer corrections) and ONIOM-EE²⁵⁻²⁸ (ONIOM with electrostatic embedding) to correct for charge transfer and electrostatic interactions, respectively. The current work aims to bring these two distinct methods together under one umbrella. Furthermore, analytic gradients of the method have been derived and implemented for the efficient optimization of structures with this method. We note that some popular methods like X-POL¹⁹ have been reformulated to enable efficient analytic gradient implementation.²⁰ In this work, our models will also be derived with a focus on the efficient implementation of the analytic gradient. The exact form of the gradient depends on the charge model. This work will employ Mulliken charge²⁹ model. This work is organized as follows. Section 2 gives background information. Section 3 presents our method. Section 4 presents the results and the corresponding discussion. Section 5 analyzes the computational cost. Section 6 summarizes our conclusions.

2. BACKGROUND

The current work aims to correct for both electrostatic interaction and charge transfer deficiencies in ONIOM. Here, we briefly describe the ONIOM-CT and ONIOM-EE methods to account for the two deficiencies individually. The difference between the methods lies in the creation of the model systems. Figure 1 presents the two methods.

Since we are combining two different methods, some notations are tweaked for ease of generalization. We will use \tilde{E} to represent the energy without embedding (both charge on link atom and/or background charges wherever applicable) contributions in an embedded calculation. μ , ν , λ , and σ will be used to represent atomic orbitals. Parameters P, S, and C will represent density matrix, overlap matrix, and MO coefficients, respectively. Parameters i, j, k, and l represent occupied orbitals, parameters a and b represent unoccupied orbitals, and parameters p and q represent general molecular orbitals. These notations are used throughout the rest of the text.

2.1. ONIOM-CT. Mayhall and Raghavachari suggested this method to correct for charge redistribution effects across the boundary of ONIOM.²³ This method places a point charge on the link atom nucleus to balance the charge in the model

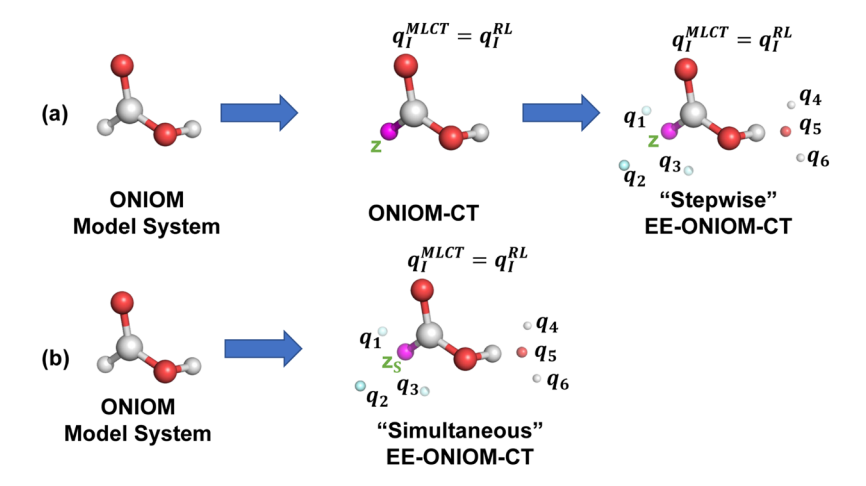


Figure 2. Process of model system preparation for (a) stepwise and (b) simultaneous models of EE-ONIOM-CT. In the case of the "stepwise" model, we first treat the charge transfer effect and later take the effect of the rest of the system while maintaining the ONIOM-CT condition. On the other hand, the "simultaneous" model takes into account both charge transfer and polarization effects simultaneously. This is performed by considering the background charges during ONIOM-CT iterations resulting in additional charge on link atoms (z_s) being different than that of regular ONIOM-CT (z).

region by pushing or pulling electrons in or out of it. ONIOM-CT has been shown to improve the performance of ONIOM using 3 different charge models, i.e., Mulliken, Löwdin, and Hirshfeld. The ONIOM-CT energy expression is given in eq 4.

$$E_{\text{ONIOM-CT}} = E_{\text{RL}} + E_{\text{MHCT}} - E_{\text{MLCT}} \tag{4}$$

 E_{MHCT} and E_{MLCT} are model region energies at high (H) and low (L) levels of theory, respectively, using charge z on the link atom satisfying the condition $q_I^{\mathrm{MLCT}} = q_I^{\mathrm{RL}}$. Here, q_I^{MLCT} and q_I^{RL} are model region charges in ML and RL calculations, respectively, in ONIOM-CT. Note that the model region does not include the link atom. We will use the notation MHCT and MLCT to represent the MH and ML calculations, respectively, using the above charge z on the link atom.

The analytic gradient of ONIOM-CT has also been developed.²⁴ In order to obtain the analytic gradient, the energy expression is written as in eq 5:

$$E_{\text{ONIOM-CT}} = E_{\text{RL}} + \tilde{E}_{\text{MHCT}} - \tilde{E}_{\text{MLCT}} + z\Delta\phi_z$$
 (5)

$$\Delta \phi_z = \phi_{\text{MHCT};z} - \phi_{\text{MLCT};z} \tag{6}$$

Here, z is the additional charge on the link atom required to satisfy the ONIOM-CT condition. The interaction of the charge on the link atom with the model system is denoted by the term $z\Delta\phi_z$, where $\Delta\phi_z$ is the difference in electrostatic potential between MH ($\phi_{\rm MHCT;z}$) and ML ($\phi_{\rm MLCT;z}$) calculations at the link atom, as per eq 6. Differentiating this expression, the analytic gradient is given as follows:

$$E_{\text{ONIOM-CT}}^{x} = E_{\text{RL}}^{x} + \tilde{E}_{\text{MHCT}}^{x} - \tilde{E}_{\text{MLCT}}^{x} + z\phi_{\text{MHCT};z}^{x}$$
$$-z\phi_{\text{MLCT};z}^{x} + z^{x}\Delta\phi_{z}$$
(7)

$$z^{x} = B \left\{ \left(\frac{dq_{I}^{RL}}{dx} \right) - \left(\frac{\partial q_{I}^{MLCT}}{\partial x} \right) \right\}$$
 (8)

where B (eq 9) represents the inverse of the response of the model region charge with respect to the link-atom nuclear charge in the ONIOM-CT calculation, and must be obtained numerically.

$$B = \left(\frac{\partial q_I^{MLCT}}{\partial z}\right)^{-1} \tag{9}$$

The analytical gradient of ONIOM-CT has been obtained for Mulliken and Löwdin charge models. For their exact expressions and a full derivation, please see ref 24.

2.2. ONIOM-EE. ONIOM-EE was initially implemented using point charges and later generalized to electronic density²⁸ as the embedding charges for the model system. The point charge implementations include Mulliken charges,²⁵ Löwdin charges²⁷ and generalized asymmetric Mulliken charges.²⁶ All of these implementations include both energy and analytic gradients. The general form of energy of ONIOM-EE methods using point charges can be conveniently written as

$$E_{\rm ONIOM\text{-}EE} = E_{\rm RL} + \tilde{E}_{\rm MH}^{\rm Emb} - \tilde{E}_{\rm ML}^{\rm Emb} + \sum_{A} q_{A} \phi_{\rm MH;A}^{\rm Emb} - \sum_{A} q_{A} \phi_{\rm ML;A}^{\rm Emb}$$

$$\tag{10}$$

where q_A is the embedded charge on atom A during model system calculations, $\phi_{\mathrm{MH};A}^{\mathrm{Emb}}$ and $\phi_{\mathrm{ML};A}^{\mathrm{Emb}}$ are the corresponding electrostatic potentials in MH and ML calculations, respectively. The last two terms in eq 10 represent the embedding potential on the model system. The above notation of using the superscript "Emb" to denote model system calculations involving embedded charges will be used throughout the rest of the text. Differentiating eq 10 gives the following analytic gradient:

$$E_{\text{ONIOM-EE}}^{x} = E_{\text{RL}}^{x} + \tilde{E}_{\text{MH}}^{\text{Emb}^{x}} - \tilde{E}_{\text{ML}}^{\text{Emb}^{x}} + \sum_{A} q_{A} \phi_{\text{MH;A}}^{\text{Emb}^{x}}$$
$$- \sum_{A} q_{A} \phi_{\text{ML;A}}^{\text{Emb}^{x}} + \sum_{A} q_{A}^{x} \phi_{\text{MH;A}}^{\text{Emb}} - \sum_{A} q_{A}^{x} \phi_{\text{ML;A}}^{\text{Emb}}$$
(11)

The final resulting exact expressions used in the implementation are dependent on the charge model. Please refer to their original papers^{2.5-2.7} for further information. We will use notations A and B to denote the locations of the embedded charges throughout the rest of the text.

2.3. Mulliken Charges. Charges on atoms are a coarsegrained representation of the electronic density, and their

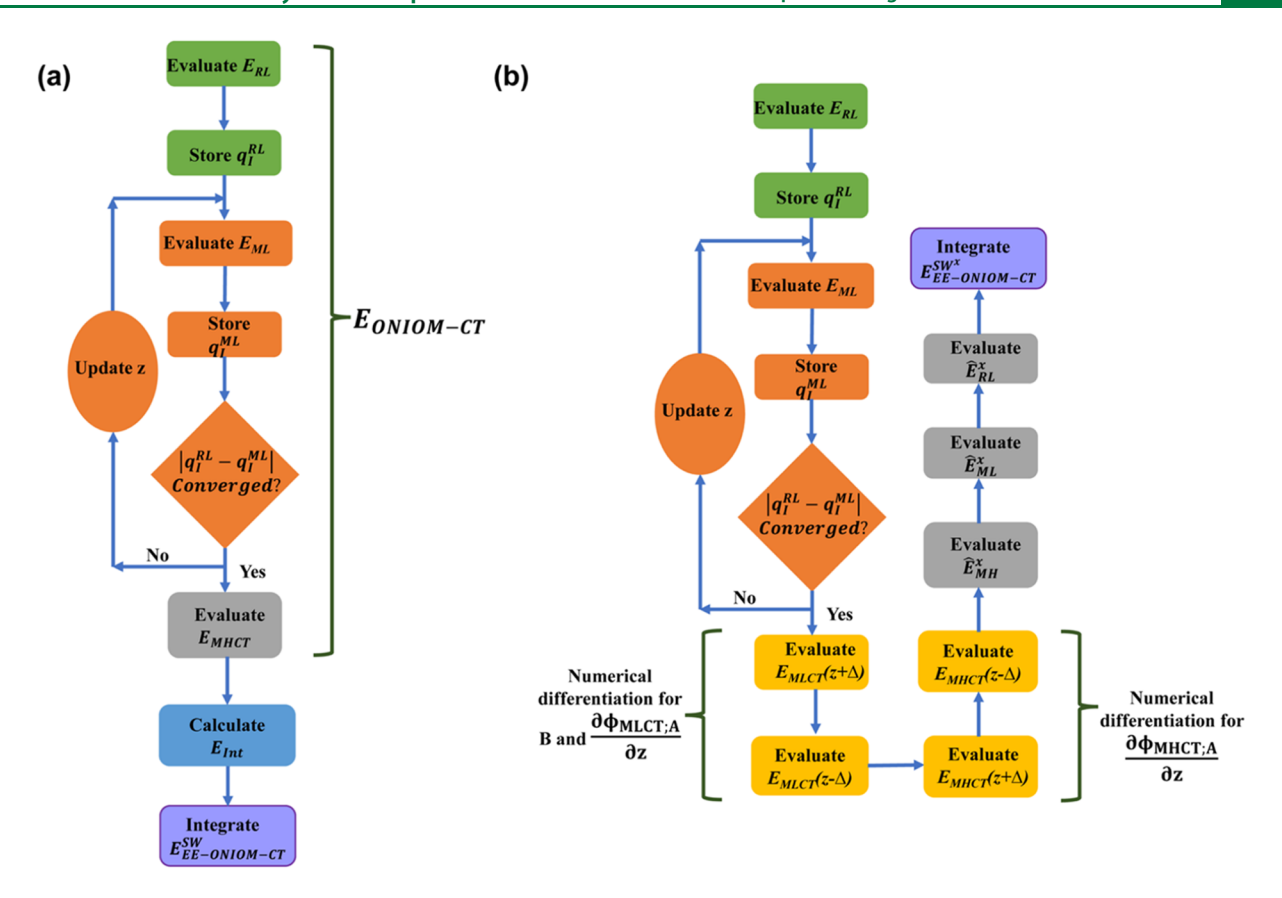


Figure 3. Flowchart for the calculation of (a) energy ($E_{\rm EE-ONIOM-CT}^{\rm SW}$) and (b) analytic gradient ($E_{\rm EE-ONIOM-CT}^{\rm SW^*}$) using the "stepwise" model. The different phases are color-coded for ease of distinction.

magnitudes are dependent on the charge model of choice. Mulliken charge model is a basis set dependent charge model that is most widely used in embedding methods²⁰ and charge balance¹⁶ purposes due to its inexpensive nature and ease of formulation of analytic gradient. We will be using this charge model in the current work. The Mulliken charge on atom $A(q_A)$ and its analytic gradient (q_A^x) are the following:

$$q_{A} = Z_{A} - \sum_{\mu \in A} \sum_{\nu} P_{\mu\nu} S_{\mu\nu} \tag{12}$$

$$q_A^x = -\sum_{\mu \in A} \sum_{\nu} \left(P_{\mu\nu}^x S_{\mu\nu} + P_{\mu\nu} S_{\mu\nu}^x \right)$$
 (13)

3. EE-ONIOM-CT METHOD

EE-ONIOM-CT method uses point charges as embedding charges and an additional charge on the link atom to balance the charge in the model region. Thus, it needs to effectively perform both ONIOM-EE and ONIOM-CT. We propose two different models to achieve this, as shown in Figure 2.

These models are called "stepwise" and "simultaneous" because of the approach used to combine ONIOM-EE and ONIOM-CT. In the following two subsections, we discuss the implementation of the two models for systems with only one link atom. However, the extension to multiple link atoms is straightforward by summing over potentials on all of the link atoms. This is enabled by our previous formulation of ONIOM-CT, which places equal charge on all the link atoms, assuming the bonds being cut are similar in nature (typically C–C bonds).²⁴ This formulation has the added

advantage of not requiring the numerical gradients with respect to the link atom charge (e.g., $\frac{\partial \phi_{\text{MHCT};A}}{\partial z}$ in eq 18) to be calculated individually, keeping the computational cost low.

3.1. "Stepwise" Model. As the name suggests, this model treats the two deficiencies in a stepwise manner by first satisfying the ONIOM-CT condition for charge balance before accounting for the electrostatic interactions from the rest of the system. This is conceptually a perturbative approach and has the advantage of easy interpretation due to the clear separation of the two effects. The energy of this model is obtained as follows.

$$E_{\text{EE-ONIOM-CT}}^{\text{SW}} = E_{\text{ONIOM-CT}} + E_{\text{Int}}$$
 (14)

$$E_{\text{Int}} = \sum_{A} q_{A} \Delta \phi_{A} \tag{15}$$

$$\Delta \phi_{\!\scriptscriptstyle A} = \phi_{\scriptscriptstyle \mathrm{MHCT;A}} - \phi_{\scriptscriptstyle \mathrm{MLCT;A}} \tag{16}$$

Here, $\phi_{\mathrm{MHCT};A}$ and $\phi_{\mathrm{MLCT};A}$ are electrostatic potentials on background charge (q_A) from unembedded MH and ML calculations, respectively, post convergence of ONIOM-CT cycle. The energy calculation can be conveniently divided into following five phases:

- (1) Perform RL calculation and extract the embedded charges (q_A) and $q_I^{\rm RL}$. This step yields $E_{\rm RL}$.
- (2) Perform ONIOM-CT cycle to obtain the appropriate charge (z) to be added to the link atom nuclear charge. In this cycle, ML calculations are performed in the absence of the background charges (q_A) on atoms in the

rest of the system. This step yields E_{MLCT} along with the electrostatic potentials on atoms of the rest of the system $(\phi_{MLCT:A})$ from ML calculation.

- (3) Next, perform MH calculation using the same charge on link atom nucleus (z) as in the MLCT calculation. This step yields E_{MHCT} along with the electrostatic potential on atoms of the rest of the system ($\phi_{\mathrm{MHCT;A}}$) from MH calculation.
- (4) The potential obtained from last two steps and the charges obtained from the first step are used to calculate E_{Int} (eq 15).
- (5) Finally, the energies from the last four steps are summed appropriately to get the EE-ONIOM-CT energy (E^{SW}_{EE-ONIOM-CT}).

The workflow to obtain the energy is presented in Figure 3a. The energy workflow resembles that of ONIOM-CT due to the interaction energy being calculated separately. However, this does not apply to the calculation of gradients which will be discussed next.

Differentiating the energy in eq 14 and using the ONIOM-CT gradient from eq 7, we get

$$\begin{split} E_{\text{EE-ONIOM-CT}}^{SW^x} &= E_{\text{RL}}^x + \tilde{E}_{\text{MHCT}}^x - \tilde{E}_{\text{MLCT}}^x + z\phi_{\text{MHCT};z}^x \\ &- z\phi_{\text{MLCT};z}^x + z^x\Delta\phi_z \\ &+ \sum_A q_A \!\! \left(\! \frac{\mathrm{d}\phi_{\text{MHCT};A}}{\mathrm{d}x} - \frac{\mathrm{d}\phi_{\text{MLCT};A}}{\mathrm{d}x} \right) + q_A^x\Delta\phi_A \end{split}$$

Since, the electrostatic potentials ($\phi_{MHCT;A}$ and $\phi_{MLCT;A}$) at q_A depend both on the coordinates and the charge on link atom (z), their gradients can be written as follows:

$$\frac{\mathrm{d}\phi_{\mathrm{MHCT;A}}}{\mathrm{d}x} = \phi_{\mathrm{MHCT;A}}^{x} + \frac{\partial\phi_{\mathrm{MHCT;A}}}{\partial z} * z^{x}$$
(18)

$$\frac{\mathrm{d}\phi_{\mathrm{MLCT;A}}}{\mathrm{d}x} = \phi_{\mathrm{MLCT;A}}^{x} + \frac{\partial\phi_{\mathrm{MLCT;A}}}{\partial z} * z^{x}$$
(19)

Using the expression of z^x from eq 8, the analytic gradient can be rewritten as follows:

$$\begin{split} E_{\text{EE-ONIOM-CT}}^{\text{SW}^x} &= E_{\text{RL}}^x + \tilde{E}_{\text{MHCT}}^x - \tilde{E}_{\text{MLCT}}^x + z \phi_{\text{MHCT};z}^x \\ &- z \phi_{\text{MLCT};z}^x + B \Bigg(\frac{\mathrm{d}q_l^{\text{RL}}}{\mathrm{d}x} \Bigg) \Delta \phi_z - B \Bigg(\frac{\partial q_l^{\text{MLCT}}}{\partial x} \Bigg) \Delta \phi_z \\ &+ \sum_A \Bigg[q_A (\phi_{\text{MHCT};A}^x - \phi_{\text{MLCT};A}^x) \\ &+ q_A \Bigg(\frac{\partial \phi_{\text{MHCT};A}}{\partial z} - \frac{\partial \phi_{\text{MLCT};A}}{\partial z} \Bigg) \\ &\times B \Bigg\{ \Bigg(\frac{\mathrm{d}q_l^{\text{RL}}}{\mathrm{d}x} \Bigg) - \Bigg(\frac{\partial q_l^{\text{MLCT}}}{\partial x} \Bigg) \Bigg\} + q_A^x \Delta \phi_A \Bigg] \end{split}$$

Rearranging eq 20, $E_{\rm EE-ONIOM-CT}^{\rm SW^*}$ can be written as follows:

$$E_{\text{EE-ONIOM-CT}}^{\text{SW}^x} = \hat{E}_{\text{RL}}^x + \hat{E}_{\text{MH}}^x - \hat{E}_{\text{ML}}^x$$
 (21)

where

$$\hat{E}_{\rm RL}^{\,x} = E_{\rm RL}^{\,x} + B' q_I^{\rm RL}^{\,x} + \sum_A q_A^{\,x} \Delta \phi_A \tag{22}$$

$$\hat{E}_{\text{MH}}^{x} = \tilde{E}_{\text{MHCT}}^{x} + z\phi_{\text{MHCT};z}^{x} + \sum_{A} q_{A}\phi_{\text{MHCT};A}^{x}$$
(23)

$$\hat{E}_{\text{ML}}^{x} = \tilde{E}_{\text{MLCT}}^{x} + z\phi_{\text{MLCT};z}^{x} + B'q_{I}^{\text{MLCT}^{x}} + \sum_{A} q_{A}\phi_{\text{MLCT};A}^{x}$$
(24)

$$B' = B \left\{ \Delta \phi_z + \sum_{A} q_A \left[\left(\frac{\partial \phi_{\text{MHCT};A}}{\partial z} - \frac{\partial \phi_{\text{MLCT};A}}{\partial z} \right) \right] \right\}$$
(25)

The terms $\frac{\partial \phi_{\text{MHCT;A}}}{\partial z}$ and $\frac{\partial \phi_{\text{MLCT;A}}}{\partial z}$ are obtained numerically. Equations 22, 23, and 24 result in three independent calculations to be summed to obtain the final gradient. The order of the calculations must be carefully determined for maximum efficiency. The procedure is performed in five phases as follows:

- (1) Perform RL calculation and extract the embedded charges (q_A) and q_I^{RL} . This step yields E_{RL} .
- (2) Perform ONIOM-CT cycle to obtain the appropriate charge (z) to be added to the link atom nuclear charge. In this cycle, ML calculations are performed in the absence of the background charges (q_A) on atoms in the rest of the system. This step yields $E_{\rm MLCT}$ along with the electrostatic potentials on atoms of the rest of the system ($\phi_{\rm MLCT:A}$) from ML calculation.
- (3) Next, perform ML calculations using a slightly modified charge on link atom $((z + \Delta) \text{ and } (z \Delta))$, to obtain B and $\frac{\partial \phi_{\text{MLCT;A}}}{\partial z}$ by symmetric finite differentiation. This is followed by analogues numerical gradient using MH calculations to compute $\frac{\partial \phi_{\text{MHCT;A}}}{\partial z}$.
- (4) The gradients for MH, ML and RL calculations are performed in that order according to eqs 22, 23, and 24, respectively. MH calculation used the same charge on link atom nucleus (z) as ML calculation.
- (5) Finally, the gradients from the last step are summed appropriately to get the EE-ONIOM-CT gradient (EEE-ONIOM-CT). An efficient workflow is designed and presented in Figure 3b.

We should note that the interaction term $(E_{\rm Int})$, required to obtain energy, is calculated during the calculation of $\hat{E}_{\rm ML}^{\rm x}$. Since $\phi_{\rm MHCT;A}$ and $\phi_{\rm MLCT;A}$ are part of the interaction, they are treated as perturbations and their explicit gradient is obtained as follows:

$$\phi_{\text{MHCT;}A}^{x} = \sum_{M} \left(\frac{Z_{M}}{R_{MA}} \right)^{x} - \sum_{\mu_{H}\nu_{H}} P_{\mu_{H}\nu_{H}} V_{\mu_{H}\nu_{H};A}^{x} + P_{\mu_{H}\nu_{H}}^{x} V_{\mu_{H}\nu_{H};A}^{x}$$
(26)

$$V_{\mu_{H}\nu_{H};A} = \langle \varphi_{\mu_{H}} | r_{1A}^{-1} | \varphi_{\nu_{H}} \rangle \tag{27}$$

$$\phi_{\text{MLCT};A}^{x} = \sum_{M} \left(\frac{Z_{M}}{R_{MA}} \right)^{x} - \sum_{\mu_{L}\nu_{L}} P_{\mu_{L}\nu_{L}} V_{\mu_{L}\nu_{L};A}^{x} + P_{\mu_{L}\nu_{L}}^{x} V_{\mu_{L}\nu_{L};A}$$
(28)

$$V_{\mu_L\nu_L;A} = \langle \varphi_{\mu_l} | r_{1A}^{-1} | \varphi_{\nu_L} \rangle \tag{29}$$

Here, Z_M is the nuclear charge on atom M and R_{MA} is its distance from the embedded charge on A. $P_{\mu_1\nu_1}$ and $P_{\mu_1\nu_1}$ are

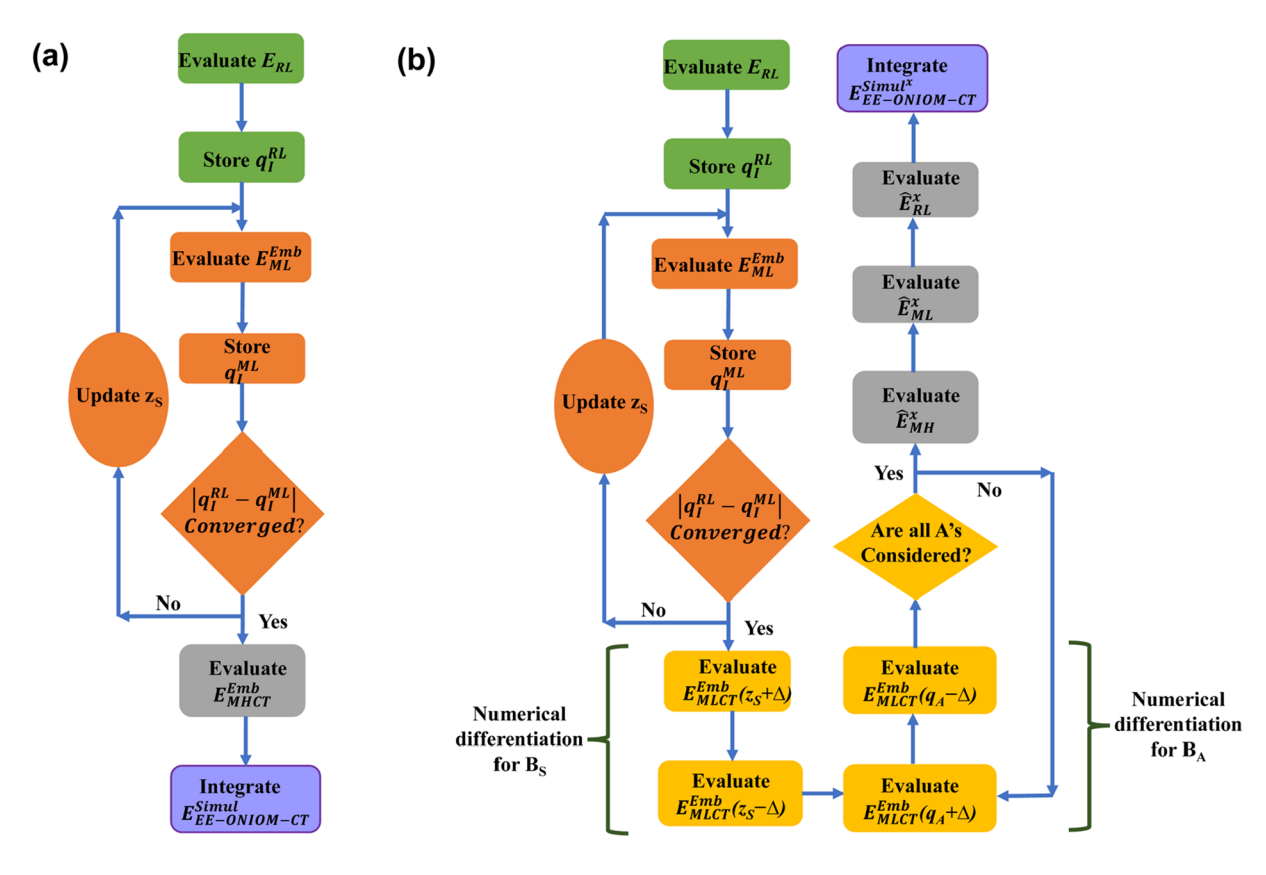


Figure 4. Flowchart for the calculation of (a) energy ($E_{\text{EE-ONIOM-CT}}^{\text{Simul}}$) and (b) analytic gradient ($E_{\text{EE-ONIOM-CT}}^{\text{Simul}^s}$) of EE-ONIOM-CT using the "simultaneous" model. The different phases are colored for ease of distinction.

MH and ML density matrices, respectively. $V_{\mu_H\nu_H;A}$ and $V_{\mu_L\nu_L;A}$ are electrostatic potentials on A from MH and ML calculations, respectively, in the AO basis. Since only the difference in electrostatic potentials between MH and ML is used, the nuclear contribution cancels out. Using eq 26 in eq 23 and eq 28 in eq 24, and assuming Mulliken charges, the final form of \hat{E}_{RL}^x , \hat{E}_{MH}^x and \hat{E}_{ML}^x take the following form.

$$\hat{E}_{RL}^{x} = E_{RL}^{x} - \sum_{\mu,\nu} P'_{\mu\nu} S_{\mu\nu}^{x}$$

$$- \sum_{\mu,\nu} S'_{\mu\nu} \left\{ \sum_{i,a} C_{\mu i} C_{\nu a} P_{ia}^{x} + \sum_{i,a} C_{\mu a} C_{\nu i} P_{ai}^{x} - \sum_{i,j} C_{\mu i} C_{\nu j} S_{ij}^{x} \right\}$$
(30)

$$P'_{\mu\nu} = \begin{cases} B'P_{\mu\nu} & \text{if } \mu \in I \\ \Delta \phi_{A} P_{\mu\nu} & \text{if } \mu \in A \\ 0 & \text{otherwise} \end{cases}$$
 (31)

$$S'_{\mu\nu} = \begin{cases} B'S_{\mu\nu} & \text{if } \mu \in I \\ \Delta \phi_A S_{\mu\nu} & \text{if } \mu \in A \\ 0 & (32) \end{cases}$$

$$\hat{E}_{ML}^{x} = \tilde{E}_{MLCT}^{x} + z\phi_{MLCT;z}^{x} \\
- B' \sum_{\mu \in I,\nu} \left\{ P_{\mu\nu} S_{\mu\nu}^{x} + S_{\mu\nu} \left(\sum_{i,a} C_{\mu i} C_{\nu a} P_{ia}^{x} + \sum_{i,a} C_{\mu a} C_{\nu i} P_{ai}^{x} \right) - \sum_{i,j} C_{\mu i} C_{\nu j} S_{ij}^{x} \right\} \\
- \sum_{i,j} \left\{ P_{\mu\nu} \left(\sum_{A} q_{A} V_{\mu\nu;A}^{x} \right) + \left(\sum_{A} q_{A} V_{\mu\nu;A} \right) \left(\sum_{i,a} C_{\mu i} C_{\nu a} P_{ia}^{x} \right) + \sum_{i,a} C_{\mu a} C_{\nu i} P_{ai}^{x} - \sum_{i,j} C_{\mu i} C_{\nu j} S_{ij}^{x} \right) \right\} \\
+ \sum_{i,a} C_{\mu a} C_{\nu i} P_{ai}^{x} - \sum_{i,j} C_{\mu i} C_{\nu j} S_{ij}^{x} \right) \\
+ \left(\sum_{A} q_{A} V_{\mu\nu;A} \right) \left(\sum_{i,a} C_{\mu i} C_{\nu a} P_{ia}^{x} + \sum_{i,a} C_{\mu a} C_{\nu i} P_{ai}^{x} - \sum_{i,j} C_{\mu i} C_{\nu j} S_{ij}^{x} \right) \right\}$$

$$- \sum_{i,j} C_{\mu i} C_{\nu j} S_{ij}^{x} \right)$$

$$(34)$$

This form of the gradient allows for the use of interchange theorem and, consequently, the z-vector method of Handy and Schaefer.³⁰ The transformation of the density matrix (P) gradient term from AO to MO basis was necessary to use the

general Post-Hartree-Fock gradient formalism.³¹ These equations are converted to a Lagrangian formalism to complete the implementation via the z-vector method. Further details can be found in the Appendix.

An efficient workflow is designed and presented in Figure 3b. Note that the gradient requires solving three sets of z-vector self-consistent equations, one each for RL, ML, and MH. In addition, one numerical gradient with respect to the extra charge on the link atom is evaluated for both ML and MH calculations. Despite the presence of these terms, we show, in Section 5, that the gradient implementation is very efficient.

Overall, the stepwise implementation allows for easy interpretation of the effects of each term (EE vs CT). Moreover, the procedure is numerically stable since the extra charge on the link atom is obtained through a previously known and well-tested method ONIOM-CT.²³

3.2. "Simultaneous" Model. This is conceptually more sophisticated and perhaps more intuitive than the stepwise model. The name "simultaneous" refers to its ability to account for both the deficiencies simultaneously as shown in Figure 2b. This is achieved by performing ONIOM-CT iterations, while embedding the model system in background charges. At convergence, the ONIOM-CT condition $(q_1^{\text{MLCT}} = q_1^{\text{RL}})$ gets satisfied while polarizing the model system using the embedded charges, as in ONIOM-EE. The energy is obtained as per eq 35.

$$E_{\text{EE-ONIOM-CT}}^{\text{Simul}} = E_{\text{RL}} + E_{\text{MHCT}}^{\text{Emb}} - E_{\text{MLCT}}^{\text{Emb}}$$
(35)

$$E_{\rm MHCT}^{\rm Emb} = \tilde{E}_{\rm MHCT}^{\rm Emb} + z_{\rm S} \phi_{\rm MHCT;z_{\rm S}}^{\rm Emb} + \sum_{A} q_{A} \phi_{\rm MHCT;A}^{\rm Emb}$$
 (36)

$$E_{\text{MLCT}}^{\text{Emb}} = \tilde{E}_{\text{MLCT}}^{\text{Emb}} + z_{\text{S}} \phi_{\text{MLCT};z_{\text{S}}}^{\text{Emb}} + \sum_{A} q_{A} \phi_{\text{MLCT};A}^{\text{Emb}}$$
(37)

Here, z_S is the extra nuclear charge placed on the link atom, $\phi_{\mathrm{MHCT};A}^{\mathrm{Emb}}$ and $\phi_{\mathrm{MHCT};Z_S}^{\mathrm{Emb}}$ are electrostatic potentials on the embedded charges (q_A) and link atom, respectively, from MH calculation and $\phi_{\mathrm{MLCT};A}^{\mathrm{Emb}}$ and $\phi_{\mathrm{MLCT};Z_S}^{\mathrm{Emb}}$ are electrostatic potentials on the embedded charges (q_A) and link atom, respectively, from ML calculation. The extra charge on the link atom, z_S , is obtained using the ONIOM-CT cycle with the model system being embedded using background charges (q_A) . We distinguish the extra charge on link atom in this model of EE-ONIOM-CT from ONIOM-CT due to the presence of embedded charges in the current ONIOM-CT cycle. The workflow followed is presented in Figure 4a.

There are two primary differences between the current and the stepwise model in the energy calculation.

- (1) No extra interaction needs to be calculated in this model.
- (2) All model system calculations are performed in the presence of embedded charges.

Given the number of iterations being equal, the computational cost of the energy calculation will be the same for both models. However, this may not hold for the gradient that will be formulated next.

The analytic gradient is obtained by differentiating the energy expression in eq 35:

$$E_{\text{EE-ONIOM-CT}}^{\text{Simul}^{x}} = E_{\text{RL}}^{x} + E_{\text{MHCT}}^{\text{Emb}^{x}} - E_{\text{MLCT}}^{\text{Emb}^{x}}$$
(38)

Using eqs 36 and 37, the gradient expression can be transformed to a more practical form, which is as shown in eq 39:

$$\begin{split} E_{\text{EE-ONIOM-CT}}^{\text{Simul}^x} &= E_{\text{RL}}^x + \tilde{E}_{\text{MHCT}}^{\text{Emb}^x} - \tilde{E}_{\text{MLCT}}^{\text{Emb}^x} + z_S \phi_{\text{MHCT};z_S}^{\text{Emb}^x} \\ &- z_S \phi_{\text{MLCT};z_S}^{\text{Emb}^x} + z_S^x \Delta \phi_{z_S}^{\text{Emb}} \\ &+ \sum_A \left(q_A \phi_{\text{MHCT};A}^{\text{Emb}^x} - q_A \phi_{\text{MLCT};A}^{\text{Emb}^x} + q_A^x \Delta \phi_A^{\text{Emb}} \right) \end{split}$$

$$\Delta \phi_{z_{S}}^{\text{Emb}} = \phi_{\text{MHCT};z_{S}}^{\text{Emb}} - \phi_{\text{MLCT};z_{S}}^{\text{Emb}}$$
(40)

$$\Delta \phi_A^{\text{Emb}} = \phi_{\text{MHCT};A}^{\text{Emb}} - \phi_{\text{MLCT};A}^{\text{Emb}} \tag{41}$$

The terms in eq 39 need to be grouped into three groups, one each representing RL, ML, and MH. This is due to the presence of only three types of calculations in two-layer ONIOM. Electrostatic potentials are one electron integrals, and their derivatives can be performed with the corresponding calculations. $\phi_{\mathrm{MHCT};z_s}^{\mathrm{Emb}^x}$ and $\phi_{\mathrm{MHCT};A}^{\mathrm{Emb}^x}$ are grouped into MH calculation, $\phi_{\mathrm{MLCT};z_s}^{\mathrm{Emb}^x}$ and $\phi_{\mathrm{MLCT};A}^{\mathrm{Emb}^x}$ are grouped into the ML calculation. Note, in this model, the electrostatic potentials of the embedded charges were present in the ML and MH Hamiltonians and do not need to be treated as perturbations. q_A^x can be performed along with RL calculation as explained in ref 25. This leaves us with the following value: z_s^x . Since, z_s is obtained using an iterative process, its gradient is nontrivial. To formulate z_s^x we will start from the convergence criterion which is as follows:

$$q_I^{\rm RL} = q_I^{\rm MLCT}(z_S; q_A) \tag{42}$$

 $q_I^{\rm MLCT}$ depends on coordinates, extra charge on link atom (z_s) and the embedded charges (q_A). Differentiating eq 42, we get

$$\frac{\mathrm{d}q_{I}^{\mathrm{RL}}}{\mathrm{d}x} = \frac{\partial q_{I}^{\mathrm{MLCT}}}{\partial x} + \frac{\partial q_{I}^{\mathrm{MLCT}}}{\partial z_{S}} * z_{S}^{x} + \sum_{A} \frac{\partial q_{I}^{\mathrm{MLCT}}}{\partial q_{A}} * q_{A}^{x}$$
(43)

eq 43 can be rearranged as follows to obtain the form of z_s^x .

$$z_{S}^{x} = B_{S} \left(\frac{\mathrm{d}q_{I}^{\mathrm{RL}}}{\mathrm{d}x} - \frac{\partial q_{I}^{\mathrm{MLCT}}}{\partial x} - \sum_{A} B_{A} * q_{A}^{x} \right)$$
(44)

$$B_{S} = \left(\frac{\partial q_{I}^{\text{MLCT}}}{\partial z_{S}}\right)^{-1} \tag{45}$$

$$B_{A} = \frac{\partial q_{I}^{\text{MLCT}}}{\partial q_{A}} \tag{46}$$

Using eq 44 in eq 39 and rearranging, the final form of $E_{\text{EE-ONIOM-CT}}^{\text{Simul}^x}$ can be written as follows:

$$E_{\text{EE-ONIOM-CT}}^{\text{Simul}^x} = \hat{E}_{\text{RL}}^x + \hat{E}_{\text{MH}}^x - \hat{E}_{\text{ML}}^x$$
 (47)

where

$$\hat{E}_{RL}^{x} = E_{RL}^{x} + \Delta \phi_{z_{S}}^{Emb} B_{S} \frac{dq_{I}^{RL}}{dx} + \sum_{A} q_{A}^{x} (\Delta \phi_{A}^{Emb} - \Delta \phi_{z_{S}}^{Emb} B_{S} B_{A})$$

$$(48)$$

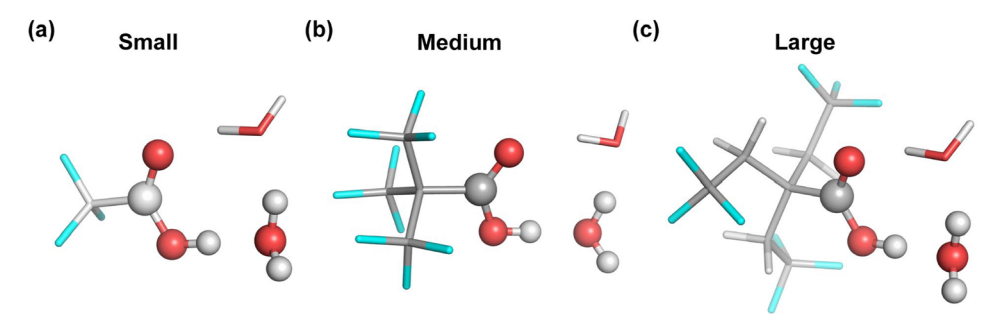


Figure 5. (a) 2,2,2-trifluoroacetic acid. $(H_2O)_2$, (b) 3,3,3-trifluoroacetic-2,2-bis(trifluoromethyl)propanoic acid. $(H_2O)_2$ and (c) 4,4,4-trifluoro-2,2-bis(2,2,2-trifluoroethyl)butanoic acid. $(H_2O)_2$ are representative molecules of different sizes to test the efficiency and veracity of our method EE-ONIOM-CT. The shown structures correspond to the first point of rigid scans illustrated in Figure 6. Model system is represented by ball and stick.

$$\hat{E}_{\text{MH}}^{x} = \tilde{E}_{\text{MHCT}}^{\text{Emb}^{x}} + z_{S} \phi_{\text{MHCT};z_{S}}^{\text{Emb}^{x}} + \sum_{A} q_{A} \phi_{\text{MHCT};A}^{\text{Emb}^{x}}$$
(49)

$$\hat{E}_{\mathrm{ML}}^{x} = \tilde{E}_{\mathrm{MLCT}}^{\mathrm{Emb}^{x}} + z_{S} \phi_{\mathrm{MLCT};z_{S}}^{\mathrm{Emb}^{x}} + \sum_{A} q_{A} \phi_{\mathrm{MLCT};A}^{\mathrm{Emb}^{x}} + \Delta \phi_{z_{S}}^{\mathrm{Emb}} B_{S} \frac{\partial q_{I}^{\mathrm{MLCT}}}{\partial x}$$
(50)

The terms B_S and B_A need to be obtained numerically. Equations 48, 49, and 50 result in three independent calculations to be summed to obtain the final gradient. Similar to the "stepwise" model, the order of the calculations must be carefully determined for maximum efficiency. The procedure is performed in five phases as follows:

- (1) Perform RL calculation and extract the embedded charges (q_A) and q_I^{RL} . This step yields E_{RL} .
- (2) Perform ONIOM-CT cycle to obtain the appropriate charge (z_S) to be added to the link atom nuclear charge. In this cycle, ML calculations are performed while keeping the background charges (q_A) on atoms in the rest of the system (except the support atom, which is substituted by the link atom) fixed. This step yields $E_{\text{MLCT}}^{\text{Emb}}$.
- (3) Next, perform a set of ML calculations, using a slightly modified charge on link atom $((z_s + \Delta) \text{ and } (z_s \Delta))$, to obtain B_S as per eq 45. This is followed by analogues numerical gradients to compute B_A corresponding to each of the embedded charges (q_A) as per eq 46.
- (4) The gradients for MH, ML, and RL calculations are performed in that order according to eqs 48, 49, and 50, respectively. MH calculation used the same background charges (q_A) and extra charge on link atom nucleus (z_S) as ML calculation.
- (5) Finally, the gradients from the last step are summed appropriately to get the EE-ONIOM-CT gradient (EEE-ONIOM-CT). An efficient workflow is designed and presented in Figure 4b.

The RL and ML calculations must be performed using the z-vector method of Handy and Schaefer.³⁰ Thus, they must be transformed from an AO to an MO basis. Using Mulliken charges and their gradient from eqs 12 and 13, exact form of RL and ML gradients can be written as follows:

$$\hat{E}_{RL}^{x} = E_{RL}^{x} - \sum_{\mu,\nu} \hat{P}_{\mu\nu} S_{\mu\nu}^{x} - \sum_{\mu,\nu} \hat{S}_{\mu\nu} \left\{ \sum_{i,a} C_{\mu i} C_{\nu a} P_{ia}^{x} + \sum_{i,a} C_{\mu a} C_{\nu i} P_{ai}^{x} - \sum_{i,j} C_{\mu i} C_{\nu j} S_{ij}^{x} \right\}$$
(51)

$$\dot{P}_{\mu\nu} = \begin{cases}
\Delta \phi_{z_S}^{\text{Emb}} B_S P_{\mu\nu} & \text{if } \mu \in I \\
(\Delta \phi_A^{\text{Emb}} - \Delta \phi_{z_S}^{\text{Emb}} B_S B_A) P_{\mu\nu} & \text{if } \mu \in A \\
0 & \text{otherwise}
\end{cases}$$
(52)

$$\dot{S}_{\mu\nu} = \begin{cases}
\Delta \phi_{z_s}^{\text{Emb}} B_S S_{\mu\nu} & \text{if } \mu \in I \\
(\Delta \phi_A^{\text{Emb}} - \Delta \phi_{z_s}^{\text{Emb}} B_S B_A) S_{\mu\nu} & \text{if } \mu \in A \\
0 & \text{otherwise}
\end{cases}$$
(53)

$$\hat{E}_{\text{ML}}^{x} = \tilde{E}_{\text{MLCT}}^{\text{Emb}^{x}} + z_{S} \phi_{\text{MLCT};z_{S}}^{\text{Emb}^{x}} + \sum_{A} q_{A} \phi_{\text{MLCT};A}^{\text{Emb}^{x}}
- \Delta \phi_{z_{S}}^{\text{Emb}} B_{S} \sum_{\mu \in I, \nu} \left\{ P_{\mu\nu} S_{\mu\nu}^{x} + S_{\mu\nu} \left(\sum_{i,a} C_{\mu i} C_{\nu a} P_{ia}^{x} \right) \right\}
+ \sum_{i,a} C_{\mu a} C_{\nu i} P_{ai}^{x} - \sum_{i,j} C_{\mu i} C_{\nu j} S_{ij}^{x} \right\}$$
(54)

These equations are converted to Lagrangian formalism to complete the implementation. Further details can be found in the Appendix.

This completes the formulation of EE-ONIOM-CT which simultaneously treats both the deficiencies, i.e., polarization and charge rearrangement of ONIOM. However, our initial exploration suggests that this model is less robust, sometimes leading to unphysical charges on the link atom, particularly if sizable quantity of external charges are present close to the regional boundary. This may be similar to the overpolarization effects commonly seen in QM/MM methods when the embedding charges are too close. In addition, our current formalism requires a numerical differentiation of the model system charge with respect to all the background charges ($B_{\rm A}$) and may be impractical for many applications. While simplifications may be possible, we have not explored them, since the method appears to be less robust. Comparison

Table 1. RMS and MAX Errors of the Analytic Gradients, with Respect to Numerical Forces^a

	RMS Force Error (au)						
	ONIOM	ONIOM-EE	ONIOM-CT	Simultaneous	Stepwise		
Small	3.09×10 ⁻⁸	3.09×10 ⁻⁸	4.27×10 ⁻⁸	3.08×10 ⁻⁸	3.51×10 ⁻⁸		
Medium	4.25×10 ⁻⁸	4.25×10 ⁻⁸	4.75×10 ⁻⁸	1.62×10 ^{-7^b}	5.46×10 ⁻⁸		
Large	1.21×10 ⁻⁸	1.21×10 ⁻⁸	4.08×10 ⁻⁸	1.23×10 ⁻⁸	4.32×10 ⁻⁸		
	MAX Force Error (au)						
	ONIOM	ONIOM-EE	ONIOM-CT	Simultaneous	Stepwise		

	MAX Force Error (au)						
	ONIOM	ONIOM-EE	ONIOM-CT	Simultaneous	Stepwise		
Small	1.01×10 ⁻⁷	1.01×10 ⁻⁷	9.20×10 ⁻⁸	1.01×10 ⁻⁷	9.60×10 ⁻⁸		
Medium	1.61×10 ⁻⁷	1.60×10 ⁻⁷	1.63×10 ⁻⁷	7.86×10 ^{-7^b}	2.11×10 ⁻⁷		
Large	5.40×10 ⁻⁸	5.50×10 ⁻⁸	1.34×10 ⁻⁷	5.50×10 ⁻⁸	1.44×10 ⁻⁷		

"All the structures are shown in Figure 5. All the calculations are performed at B3LYP/6-31+G(d):HF/3-21G level of theory. The terms "simultaneous" and "stepwise" represent the corresponding models of EE-ONIOM-CT. Numerical gradients were obtained using a five-point method. The RMS and MAX errors consider gradients in all three directions of all the atoms. SCF convergence criteria were set to 10^{-12} and 10^{-10} on RMS and maximum change in density. Z-vector convergence on C1(I,A) contributions is set to 10^{-12} for RMS and 10^{-11} for maximum. Default numerical gradient step size was used (0.01 Å). Numerical gradient step size was reduced to 0.001 Å.

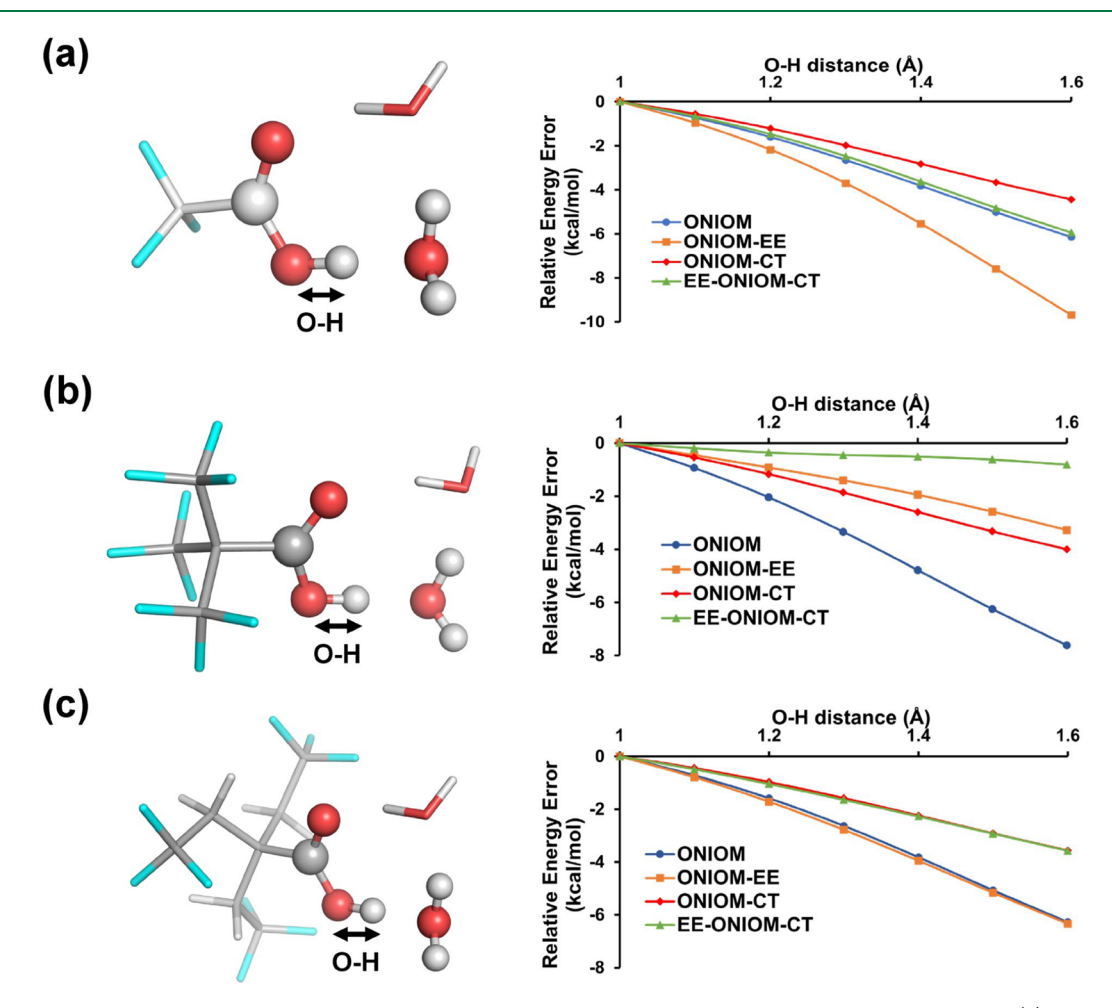


Figure 6. Rigid scans performed to study O-H dissociation. Three cases representing embedded charges being located (a) close, (b) moderate, and (c) farther away from the model system (model region represented in ball and stick). The relative energy errors are with respect to full system calculation at high level (B3LYP/6-31+G(d)) theory. All of the calculations are performed at the B3LYP/6-31+G(d):HF/3-21G level theory.

between the charge on link atom for the two models and their performance is presented in the Supporting Information.

The above issues are not present in the "stepwise" model described earlier. Additionally, in the "stepwise" model, the numerical gradients with respect to all the embedded charges

are replaced by only one numerical gradient using MH calculations. Thus, for the applications considered in this paper, the stepwise model will be considered the default model for performing EE-ONIOM-CT.

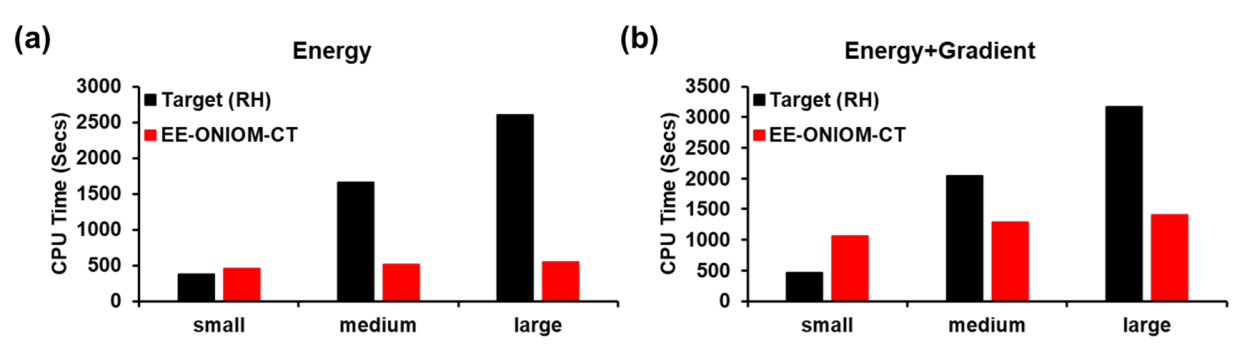


Figure 7. Computation cost comparison between the target (full system calculation at a high level theory) and EE-ONIOM-CT. EE-ONIOM-CT calculations are performed at B3LYP/6-31+G(d):HF/3-21G level theory. Thus, the target is full system calculation at B3LYP/6-31+G(d):HF/3-21G level theory.

$$E_{\text{EE-ONIOM-CT}} = E_{\text{EE-ONIOM-CT}}^{\text{SW}} \tag{55}$$

$$E_{\text{EE-ONIOM-CT}}^{x} = E_{\text{EE-ONIOM-CT}}^{\text{SW}^{x}}$$
 (56)

3.3. Check for Correctness. Both models, $E_{\rm EE-ONIOM-CT}^{\rm SW}$ and $E_{\rm EE-ONIOM-CT}^{\rm Simul}$, were implemented in a development version of Gaussian. During implementation, the transformed density matrices ($P'_{\mu\nu}$ and $\hat{P}_{\mu\nu}$) and transformed overlap matrices ($S'_{\mu\nu}$ and $\hat{S}_{\mu\nu}$) were symmetrized to allow for the use of available utilities. This is clearly evident from the expressions in the Appendix. The analytic gradients were tested against numerical gradients using the five-point method. Three molecules are used, as shown in Figure 5. The molecules are labeled small, medium, and large, to test the computational efficiency of our method (vide infra).

These molecules also correspond to the first point of the rigid scans discussed in the next section. The errors of the analytic gradients with respect to the numerical gradients are presented in Table 1. In addition to our method EE-ONIOM-CT, we also present the corresponding errors for the other well-known method, i.e., ONIOM, for scale. From the small errors we can infer that our implementation is correct.

4. RESULTS AND DISCUSSION

Since EE-ONIOM-CT is a combination of two methods, our focus will be concentrated on probing the degree of importance of the two methods under different circumstances. All of the EE-ONIOM-CT calculations illustrated in this section use the "stepwise" model. The disentanglement of the two effects in the "stepwise" model enables analysis of the effect of electrostatic embedding separately. In order to demonstrate this, we chose three different systems with embedded charges being close, at a medium distance, and farther away from the model region, as designated in Figure 5 as small, medium, and large, respectively.

We studied the O–H dissociation in all three cases using a rigid scan starting from an O–H bond length of 1.0 to 1.6 Å. The rigid scan kept the rest of the system frozen. The starting geometry was obtained by optimizing the molecule at the target level (B3LYP/6-31+G(d)). All the hybrid calculations were carried out at the B3LYP/6-31+G(d):HF/3-21G level of theory. To avoid the tendency of Mulliken charges becoming unphysical, ³² the small 3-21G basis set was used at the low-level. Small basis sets have the additional benefit of keeping the computational cost low (vide infra). The relative energy errors are listed in Figure 6. The errors are with respect to full system calculation at the target level with the first point of the scan being the reference.

In all three cases, ONIOM-CT provides an improvement over ONIOM, but the effect of electronic embedding depends on the location of the embedding charges relative to the regional boundary. In the first case ("Small"), the highly charged F atoms are connected to the host atom (i.e., the C atom is replaced by the link atom). The proximity of the embedding charges to the boundary results in overpolarization of the model system, as commonly observed in QM/MM studies. This is evident from the degradation of performance when using electrostatic embedding in Figure 6a, i.e., ONIOM-EE and EE-ONIOM-CT perform worse than ONIOM and ONIOM-CT, respectively. The second molecule ("Medium") has fluorine atoms one bond away from the host atom. The influence of the embedded charges on fluorine atoms is screened by the embedded charge on the carbon atom. This results in significant improvement in performance using electrostatic embedding as shown in Figure 6b, i.e., ONIOM-EE and EE-ONIOM-CT perform better than ONIOM and ONIOM-CT, respectively. The errors also appear to be quite low throughout the scan. In case of third molecule ("large"), the fluorine atoms are farther away from the model system and have very little influence, as shown by ONIOM-EE and EE-ONIOM-CT performance being only marginally different from ONIOM and ONIOM-CT, respectively, in Figure 6c. In this case, it appears that the effect of electrostatic embedding is similar between the high and low levels of theory and is mostly canceled. Overall, charges too close to the model system boundary have a stronger influence and need careful treatment. These results suggest that the hybrid method ONIOM is robust due to cancellation of error, but the region in proximity of the boundary can have significant influence on its performance and need careful treatment.

5. COMPUTATIONAL COST ANALYSIS

Energy and force calculations are performed on all three systems in Figure 5. Comparison between the computational cost of the target level of theory (full system calculation at high level) and EE-ONIOM-CT using the "stepwise" model is presented in Figure 7. Three different sizes of systems clearly delineate the importance of keeping the model system size small, compared to the full system to harvest the full potential of EE-ONIOM-CT. The energy calculation is extremely efficient compared to the target as shown by speedups of 3 and 5 times for "medium" and "large" systems in Figure 7a. The corresponding improvements are smaller for analytic gradients due to the greater number of steps involved. However, it is important to note that EE-ONIOM-CT force

calculations are efficient for "medium" and "large" systems with greater than 2-fold speedup for the latter. Furthermore, the increase in EE-ONIOM-CT computational cost from the "medium" to "large" systems is marginal, unlike the full calculation, and the expected speedups will be much larger as the molecular size increases. In addition, when the model system is small relative to the full molecule and a smaller basis set is used as the low level, the performance is expected to be optimal. Overall, the EE-ONIOM-CT method will be efficient for many practical applications on larger molecules since the model systems in such cases are often much smaller than the full system.

6. CONCLUSIONS

We presented our method EE-ONIOM-CT which brings together two separate methods, ONIOM-CT and ONIOM-EE under one umbrella and accounts for both charge rearrangement and electrostatic interactions. The use of a "stepwise" model was found to be necessary for a stable ONIOM-CT cycle and efficient EE-ONIOM-CT analytic gradient. The analytic gradient required solving three sets of z-vector self-consistent equations: one for the full system at the low level and one each for the model system at low-level and high-level. A detailed derivation is provided in the text. We have implemented this method efficiently and shown significant speedup relative to the full calculations.

In addition to efficient analytic gradients, the stepwise implementation disentangles the effects of charge rearrangement and electrostatic interactions, enabling the study of the influence of electrostatic embedding on chemical processes. We used a set of three proton transfer reactions to analyze the effects. While charge redistribution provides an improvement in all cases, the effects of electrostatic embedding depend on the proximity of the embedding charges to the model system boundary. Our three examples illustrate the different possibilities, involving positive, negative, and very little impact of electrostatic embedding. The broader impact of embedded charges will be a topic of discussion in future publications.

APPENDIX

The generalized post-SCF gradient needs to be written in the following form:

$$E^{x} = \sum_{\mu\nu\lambda\sigma} \Gamma_{\mu\nu\lambda\sigma}^{\text{eff}} (\mu\nu\lambda\sigma)^{x} + \sum_{\mu\nu} P_{\mu\nu}^{\text{eff}} H_{\mu\nu}^{x} + \sum_{\mu\nu} W_{\mu\nu}^{\text{eff}} S_{\mu\nu}^{x}$$

$$+V_{\text{nuc}}^{x}$$
 (A1)

$$\Gamma_{\mu\nu\lambda\sigma}^{\text{eff}} = P_{\mu\nu}^{\Delta} P_{\lambda\sigma}^{\text{SCF}} - P_{\mu\sigma}^{\Delta} P_{\lambda\nu}^{\text{SCF}}$$
(A2)

$$P_{\mu\nu}^{\rm eff} = P_{\mu\nu}^{\rm SCF} + P_{\mu\nu}^{\Delta} \tag{A3}$$

$$W_{\mu\nu}^{\text{eff}} = W_{\mu\nu}^{\text{SCF}} + W_{\mu\nu}^{\Delta} \tag{A4}$$

where $P_{\mu\nu}^{\rm SCF}$ and $W_{\mu\nu}^{\rm SCF}$ are HF or DFT density and energy weighted density matrix, respectively. $P_{\mu\nu}^{\Delta}$ and $W_{\mu\nu}^{\Delta}$ are corrections to the density and energy weighted density matrix, respectively.

It is convenient to define the corrections in the orthonormal MO basis

$$P_{\mu\nu}^{\Delta} = \sum_{pq} C_{\mu p} C_{\nu q} P_{pq}^{\Delta} \tag{A5}$$

$$P_{ij}^{\Delta} = 0 \tag{A6}$$

$$P_{ab}^{\Delta} = 0 \tag{A7}$$

Both the occupied-occupied (oo) and virtual—virtual (vv) blocks of the density matrix correction are zero. The occupied-virtual (ov) block needs solving a single set of SCF response equation:

$$\sum_{bj} [(ij||ab) - (ib||ja)] P_{bj}^{\Delta} + (\varepsilon_a - \varepsilon_i) P_{ai}^{\Delta} = L_{ai}$$
(A8)

The exact form of L_{ai} depends on the model used for EE-ONIOM-CT.

"Stepwise" Model

For RL.

$$L_{ai} = -\sum_{\mu,\nu} S'_{\mu\nu} (C_{\mu i} C_{\nu a} + C_{\mu a} C_{\nu i})$$
(A9)

For ML,

$$L_{ai} = -B' \sum_{\mu \in I, \nu} S_{\mu\nu} (C_{\mu i} C_{\nu a} + C_{\mu a} C_{\nu i})$$

$$- \sum_{\mu, \nu} \left(\sum_{A} q_{A} V_{\mu\nu; A} \right) (C_{\mu i} C_{\nu a} + C_{\mu a} C_{\nu i})$$
(A10)

For MH.

$$L_{ai} = -\sum_{\mu,\nu} \left(\sum_{A} q_{A} V_{\mu\nu;A} \right) (C_{\mu i} C_{\nu a} + C_{\mu a} C_{\nu i})$$
(A11)

"Simultaneous" Model

For RL

$$L_{ai} = -\sum_{\mu,\nu} \hat{S}_{\mu\nu} (C_{\mu i} C_{\nu a} + C_{\mu a} C_{\nu i})$$
(A12)

For ML

$$L_{ai} = -\Delta \phi_{z_s}^{\text{Emb}} B_S \sum_{\mu \in I, \nu} S_{\mu\nu} (C_{\mu i} C_{\nu a} + C_{\mu a} C_{\nu i})$$
(A13)

The energy weighted density matrix corrections will also depend on the model under consideration. Thus, we will formulate them separately.

"Stepwise" Model

$$\overline{W}_{ai}^{\Delta} = -P_{ai}^{\Delta} \varepsilon_i \tag{A14}$$

$$\overline{W}_{ab}^{\Delta} = 0 \tag{A15}$$

For RL,

$$W_{\mu\nu}^{\Delta} = \begin{cases} -B' P_{\mu\nu}^{\text{SCF}} + \sum_{pq} C_{\mu p} C_{\nu q} \overline{W}_{pq}^{\Delta} & \mu \in I \text{ and } \nu \in I \\ -\frac{1}{2} (B' + \Delta \phi_{A}) P_{\mu\nu}^{\text{SCF}} + \sum_{pq} C_{\mu p} C_{\nu q} \overline{W}_{pq}^{\Delta} & \mu \in I \text{ and } \nu \in A \text{ or } \mu \in A \text{ and } \nu \in I \end{cases}$$

$$W_{\mu\nu}^{\Delta} = \begin{cases} -\frac{1}{2} (\Delta \phi_{A} + \Delta \phi_{B}) P_{\mu\nu}^{\text{SCF}} + \sum_{pq} C_{\mu p} C_{\nu q} \overline{W}_{pq}^{\Delta} & \mu \in A \text{ and } \nu \in B \\ -\frac{1}{2} \Delta \phi_{A} P_{\mu\nu}^{\text{SCF}} + \sum_{pq} C_{\mu p} C_{\nu q} \overline{W}_{pq}^{\Delta} & \mu \in A \text{ or } \nu \in A \end{cases}$$

$$\sum_{pq} C_{\mu p} C_{\nu q} \overline{W}_{pq}^{\Delta} \qquad \text{otherwise}$$

$$(A16)$$

$$\overline{W}_{ij}^{\Delta} = \begin{cases} B' \sum_{\mu\nu} S_{\mu\nu} C_{\mu i} C_{\nu j} - \sum_{ak} P_{ak}^{\Delta}(aj||ki) & \mu \in I \text{ and } \nu \in I \\ \frac{1}{2} (B' + \Delta \phi_A) \sum_{\mu\nu} S_{\mu\nu} C_{\mu i} C_{\nu j} - \sum_{ak} P_{ak}^{\Delta}(aj||ki) & \mu \in I \text{ and } \nu \in A \text{ or } \mu \in A \text{ and } \nu \in I \end{cases}$$

$$\overline{W}_{ij}^{\Delta} = \begin{cases} \frac{1}{2} (\Delta \phi_A + \Delta \phi_B) \sum_{\mu\nu} S_{\mu\nu} C_{\mu i} C_{\nu j} - \sum_{ak} P_{ak}^{\Delta}(aj||ki) & \mu \in A \text{ and } \nu \in B \end{cases}$$

$$\frac{1}{2} \Delta \phi_A \sum_{\mu\nu} S_{\mu\nu} C_{\mu i} C_{\nu j} - \sum_{ak} P_{ak}^{\Delta}(aj||ki) & \mu \in A \text{ or } \nu \in A$$

$$-\sum_{ak} P_{ak}^{\Delta}(aj||ki) & \text{otherwise} \end{cases}$$

$$(A17)$$

For ML,

$$W_{\mu\nu}^{\Delta} = \begin{cases} -B' P_{\mu\nu}^{\text{SCF}} + \sum_{pq} C_{\mu p} C_{\nu q} \overline{W}_{pq}^{\Delta} & \mu \in I \text{ and } \nu \in I \\ -\frac{1}{2} B' P_{\mu\nu}^{\text{SCF}} + \sum_{pq} C_{\mu p} C_{\nu q} \overline{W}_{pq}^{\Delta} & \mu \in I \text{ or } \nu \in I \\ \sum_{pq} C_{\mu p} C_{\nu q} \overline{W}_{pq}^{\Delta} & \text{otherwise} \end{cases}$$
(A18)

$$\overline{W}_{ij}^{\Delta} = \begin{cases} \sum_{\mu\nu} \left(B' S_{\mu\nu} + \sum_{A} q_{A} V_{\mu\nu;A} \right) C_{\mu i} C_{\nu j} - \sum_{ak} P_{ak}^{\Delta}(aj||ki) & \mu \in I \text{ and } \nu \in I \end{cases}$$

$$\overline{W}_{ij}^{\Delta} = \begin{cases} \sum_{\mu\nu} \left(\frac{1}{2} B' S_{\mu\nu} + \sum_{A} q_{A} V_{\mu\nu;A} \right) C_{\mu i} C_{\nu j} - \sum_{ak} P_{ak}^{\Delta}(aj||ki) & \mu \in I \text{ or } \nu \in I \end{cases}$$

$$\sum_{\mu\nu} \sum_{A} q_{A} V_{\mu\nu;A} C_{\mu i} C_{\nu j} - \sum_{ak} P_{ak}^{\Delta}(aj||ki) & \text{otherwise} \end{cases}$$
(A19)

For MH,

$$\overline{W}_{ij}^{\Delta} = \sum_{\mu\nu} \sum_{A} q_{A} V_{\mu\nu;A} C_{\mu i} C_{\nu j} - \sum_{ak} P_{ak}^{\Delta}(aj||ki)$$
(A21)

$$W^{\Delta}_{\mu\nu} = \sum_{pq} C_{\mu p} C_{\nu q} \overline{W}^{\Delta}_{pq}$$
 "Simultaneous" Model
$$\overline{W}^{\Delta}_{ai} = -P^{\Delta}_{ai} \varepsilon_{i}$$
 (A22)

$$\overline{W}_{ab}^{\Delta} = 0$$
 (A23) For RL,

$$W_{\mu\nu}^{\Delta} = \begin{cases} -\Delta\phi_{z_{S}}^{\text{Emb}}B_{S}P_{\mu\nu}^{\text{SCF}} + \sum_{pq}C_{\mu p}C_{\nu q}\overline{W}_{pq}^{\Delta} & \mu \in I \text{ and } \nu \in I \\ -\frac{1}{2}(\Delta\phi_{z_{S}}^{\text{Emb}}B_{S} + (\Delta\phi_{A}^{\text{Emb}} - \Delta\phi_{z_{S}}^{\text{Emb}}B_{S}B_{A}))P_{\mu\nu}^{\text{SCF}} + \sum_{pq}C_{\mu p}C_{\nu q}\overline{W}_{pq}^{\Delta} & \mu \in I \text{ and } \nu \in A \text{ or } \mu \in A \text{ and } \nu \in I \end{cases}$$

$$W_{\mu\nu}^{\Delta} = \begin{cases} -\frac{1}{2}((\Delta\phi_{A}^{\text{Emb}} - \Delta\phi_{z_{S}}^{\text{Emb}}B_{S}B_{A}) + (\Delta\phi_{B}^{\text{Emb}} - \Delta\phi_{z_{S}}^{\text{Emb}}B_{S}B_{B}))P_{\mu\nu}^{\text{SCF}} + \sum_{pq}C_{\mu p}C_{\nu q}\overline{W}_{pq}^{\Delta} & \mu \in A \text{ and } \nu \in B \\ -\frac{1}{2}(\Delta\phi_{A}^{\text{Emb}} - \Delta\phi_{z_{S}}^{\text{Emb}}B_{S}B_{A})P_{\mu\nu}^{\text{SCF}} + \sum_{pq}C_{\mu p}C_{\nu q}\overline{W}_{pq}^{\Delta} & \mu \in A \text{ or } \nu \in A \end{cases}$$

$$\sum_{pq}C_{\mu p}C_{\nu q}\overline{W}_{pq}^{\Delta} & \text{otherwise}$$

$$(A24)$$

$$\overline{W}_{ij}^{\Delta} = \begin{cases} \Delta \phi_{z_S}^{Emb} B_S \sum_{\mu\nu} S_{\mu\nu} C_{\mu i} C_{\nu j} - \sum_{ak} P_{ak}^{\Delta}(aj|ki) & \mu \in I \text{ and } \nu \in I \\ \frac{1}{2} (\Delta \phi_{z_S}^{Emb} B_S + (\Delta \phi_A^{Emb} - \Delta \phi_{z_S}^{Emb} B_S B_A)) \sum_{\mu\nu} S_{\mu\nu} C_{\mu i} C_{\nu j} - \sum_{ak} P_{ak}^{\Delta}(aj|ki) & \mu \in I \text{ and } \nu \in A \text{ or } \mu \in A \text{ and } \nu \in I \end{cases}$$

$$\overline{W}_{ij}^{\Delta} = \begin{cases} \frac{1}{2} ((\Delta \phi_A^{Emb} - \Delta \phi_{z_S}^{Emb} B_S B_A) + (\Delta \phi_B^{Emb} - \Delta \phi_{z_S}^{Emb} B_S B_B)) \sum_{\mu\nu} S_{\mu\nu} C_{\mu i} C_{\nu j} - \sum_{ak} P_{ak}^{\Delta}(aj|ki) & \mu \in A \text{ and } \nu \in B \end{cases}$$

$$\frac{1}{2} (\Delta \phi_A^{Emb} - \Delta \phi_{z_S}^{Emb} B_S B_A) \sum_{\mu\nu} S_{\mu\nu} C_{\mu i} C_{\nu j} - \sum_{ak} P_{ak}^{\Delta}(aj|ki) & \mu \in A \text{ or } \nu \in A \end{cases}$$

$$-\sum_{ak} P_{ak}^{\Delta}(aj|ki) & \text{otherwise}$$

$$(A25)$$

For ML,

$$W_{\mu\nu}^{\Delta} = \begin{cases} -\Delta \phi_{z_{S}}^{\text{Emb}} B_{S} P_{\mu\nu}^{\text{SCF}} + \sum_{pq} C_{\mu p} C_{\nu q} \overline{W}_{pq}^{\Delta} & \mu \in I \text{ and } \nu \in I \\ -\frac{1}{2} \Delta \phi_{z_{S}}^{\text{Emb}} B_{S} P_{\mu\nu}^{\text{SCF}} + \sum_{pq} C_{\mu p} C_{\nu q} \overline{W}_{pq}^{\Delta} & \mu \in A \text{ or } \nu \in A \end{cases}$$

$$\sum_{pq} C_{\mu p} C_{\nu q} \overline{W}_{pq}^{\Delta} \qquad \text{otherwise}$$
(A26)

$$\overline{W}_{ij}^{\Delta} = \begin{cases} \Delta \phi_{z_s}^{\text{Emb}} B_S \sum_{\mu\nu} S_{\mu\nu} C_{\mu i} C_{\nu j} - \sum_{ak} P_{ak}^{\Delta}(aj||ki) & \mu \in I \text{ and } \nu \in I \end{cases}$$

$$\overline{W}_{ij}^{\Delta} = \begin{cases} \frac{1}{2} \Delta \phi_{z_s}^{\text{Emb}} B_S \sum_{\mu\nu} S_{\mu\nu} C_{\mu i} C_{\nu j} - \sum_{ak} P_{ak}^{\Delta}(aj||ki) & \mu \in A \text{ or } \nu \in A \end{cases}$$

$$-\sum_{ak} P_{ak}^{\Delta}(aj||ki) & \text{otherwise}$$

$$(A27)$$

For more information on how these equations are

ASSOCIATED CONTENT

5 Supporting Information

The Supporting Information is available free of charge at

https://pubs.acs.org/doi/10.1021/acs.jctc.3c00497.

Comparison of the performance of the two models of EE-ONIOM-CT (PDF)

AUTHOR INFORMATION

Corresponding Authors

Krishnan Raghavachari — Department of Chemistry, Indiana University, Bloomington, Indiana 47405, United States; orcid.org/0000-0003-3275-1426; Email: kraghava@indiana.edu

Vikrant Tripathy — Department of Chemistry, Indiana University, Bloomington, Indiana 47405, United States; orcid.org/0000-0002-3246-0680; Email: vtripath@iu.edu

Complete contact information is available at: https://pubs.acs.org/10.1021/acs.jctc.3c00497

Notes

The authors declare no competing financial interest.

ACKNOWLEDGMENTS

We acknowledge financial support from the National Science Foundation (Grant No. CHE-2102583) at Indiana University. The Big Red 3 supercomputing facility at Indiana University was used for most of the calculations in this study.

REFERENCES

- (1) Warshel, A.; Levitt, M. Theoretical studies of enzymic reactions: Dielectric, electrostatic and steric stabilization of carbonium ion in reaction of lysozyme. *J. Mol. Biol.* **1976**, *103*, 227–249.
- (2) Senn, H. M.; Thiel, W. QM/MM methods for biomolecular systems. *Angew. Chem. Int. Edit* **2009**, *48*, 1198–1229.
- (3) Field, M. J.; Bash, P. A.; Karplus, M. A combined quantum mechanical and molecular mechanical potential for molecular dynamics simulations. *J. Comput. Chem.* **1990**, *11*, 700–733.
- (4) Buey, M. Y.; Mineva, T.; Rapacioli, M., Coupling density functional based tight binding with class 1 force fields in a hybrid QM/MM scheme. *Theor. Chem. Acc.* **2022**, *141*. DOI: 10.1007/s00214-022-02878-6
- (5) Ferre, N.; Assfeld, X.; Rivail, J. L. Specific force field parameters determination for the hybrid ab initio QM/MM LSCF method. *J. Comput. Chem.* **2002**, 23, 610–624.
- (6) Maseras, F.; Morokuma, K. IMOMM A new integrated ab-Initio + molecular mechanics geometry optimization scheme of equilibrium structures and transition states. *J. Comput. Chem.* **1995**, 16, 1170–1179.
- (7) Humbel, S.; Sieber, S.; Morokuma, K. The IMOMO method: Integration of different levels of molecular orbital approximations for geometry optimization of large systems: Test for n-butane conformation and S(N)2 reaction: RCl+Cl-. *J. Chem. Phys.* 1996, 105, 1959–1967.
- (8) Svensson, M.; Humbel, S.; Froese, R. D. J.; Matsubara, T.; Sieber, S.; Morokuma, K. ONIOM: A Multilayered Integrated MO + MM Method for Geometry Optimizations and Single Point Energy Predictions. A Test for Diels-Alder Reactions and Pt(P(t-Bu)₃)₂+H₂ Oxidative Addition. *J. Phys. Chem-Us* 1996, 100, 19357–19363.
- (9) Chung, L. W.; Sameera, W. M. C.; Ramozzi, R.; Page, A. J.; Hatanaka, M.; Petrova, G. P.; Harris, T. V.; Li, X.; Ke, Z. F.; Liu, F. Y.; Li, H. B.; Ding, L. N.; Morokuma, K. The ONIOM Method and Its Applications. *Chem. Rev.* **2015**, *115*, 5678–5796.
- (10) Vreven, T.; Morokuma, K. On the application of the IMOMO (integrated molecular orbital + molecular orbital) method. *J. Comput. Chem.* **2000**, *21*, 1419–1432.

- (11) Field, M. J. Hybrid quantum mechanical/molecular mechanical fluctuating charge models for condensed phase simulations. *Mol. Phys.* **1997**, *91*, 835–845.
- (12) Rick, S. W.; Stuart, S. J.; Berne, B. J. Dynamical fluctuating charge force fields: Application to liquid water. *J. Chem. Phys.* **1994**, *101*, 6141–6156.
- (13) Rappe, A. K.; Goddard, W. A. Charge equilibration for molecular dynamics simulations. *J. Phys. Chem-US* **1991**, *95*, 3358–3363.
- (14) Gao, J. L. Toward a molecular orbital derived empirical potential for liquid simulations. *J. Phys. Chem. B* **1997**, *101*, 657–663. (15) Thery, V.; Rinaldi, D.; Rivail, J. L.; Maigret, B.; Ferenczy, G. G. Quantum mechanical computations on very large molecular systems: The local self-consistent field method. *J. Comput. Chem.* **1994**, *15*, 269–282.
- (16) Wang, B.; Truhlar, D. G. Combined Quantum Mechanical and Molecular Mechanical Methods for Calculating Potential Energy Surfaces: Tuned and Balanced Redistributed-Charge Algorithm. *J. Chem. Theor. Comput.* **2010**, *6*, 359–369.
- (17) Nasluzov, V. A.; Ivanova, E. A.; Shor, A. M.; Vayssilov, G. N.; Birkenheuer, U.; Rosch, N. Elastic Polarizable Environment Cluster Embedding Approach for Covalent Oxides and Zeolites Based on a Density Functional Method. *J. Phys. Chem. B* **2003**, *107*, 2228–2241.
- (18) Gao, J. L.; Amara, P.; Alhambra, C.; Field, M. J. A generalized hybrid orbital (GHO) method for the treatment of boundary atoms in combined QM/MM calculations. *J. Phys. Chem. A* **1998**, *102*, 4714–4721.
- (19) Xie, W. S.; Gao, J. L. The Design of a Next Generation Force Field: The X-POL Potential. *J. Chem. Theor. Comput.* **2007**, *3*, 1890–1900
- (20) Xie, W. S.; Song, L. C.; Truhlar, D. G.; Gao, J. L. The variational explicit polarization potential and analytical first derivative of energy: Towards a next generation force field. *J. Chem. Phys.* **2008**, 128, 234108 DOI: 10.1063/1.2936122.
- (21) Kitaura, K.; Ikeo, E.; Asada, T.; Nakano, T.; Uebayasi, M. Fragment molecular orbital method: an approximate computational method for large molecules. *Chem. Phys. Lett.* **1999**, *313*, 701–706.
- (22) Tripathy, V.; Saha, A.; Raghavachari, K. Electrostatically embedded molecules-in-molecules approach and its application to molecular clusters. *J. Comput. Chem.* **2021**, 42, 719–734.
- (23) Mayhall, N. J.; Raghavachari, K. Charge Transfer Across ONIOM QM:QM Boundaries: The Impact of Model System Preparation. J. Chem. Theor. Comput. 2010, 6, 3131–3136.
- (24) Tripathy, V.; Mayhall, N. J.; Raghavachari, K. ONIOM Method with Charge Transfer Corrections (ONIOM-CT): Analytic Gradients and Benchmarking. *J. Chem. Theor. Comput.* **2022**, *18*, 6052–6064.
- (25) Hratchian, H. P.; Parandekar, P. V.; Raghavachari, K.; Frisch, M. J.; Vreven, T. QM: QM electronic embedding using Mulliken atomic charges: Energies and analytic gradients in an ONIOM framework. J. Chem. Phys. 2008, 128, 034107.
- (26) Parandekar, P. V.; Hratchian, H. P.; Raghavachari, K. Applications and assessment of QM:QM electronic embedding using generalized asymmetric Mulliken atomic charges. *J. Chem. Phys.* **2008**, 129, 145101 DOI: 10.1063/1.2976570.
- (27) Mayhall, N. J.; Raghavachari, K.; Hratchian, H. P. ONIOMbased QM:QM electronic embedding method using Lowdin atomic charges: Energies and analytic gradients. *J. Chem. Phys.* **2010**, *132*, 114107.
- (28) Hratchian, H. P.; Krukau, A. V.; Parandekar, P. V.; Frisch, M. J.; Raghavachari, K. QM:QM embedding using electronic densities within an ONIOM framework: Energies and analytic gradients. *J. Chem. Phys.* **2011**, *135*, 014105 DOI: 10.1063/1.3603450.
- (29) Mulliken, R. S. Electronic Population Analysis on LCAO-MO Molecular Wave Functions. I. J. Chem. Phys. 1955, 23, 1833–1840.
- (30) Handy, N. C.; Schaefer, H. F. On the evaluation of analytic energy derivatives for correlated wave functions. *J. Chem. Phys.* **1984**, *81*, 5031–5033.
- (31) Frisch, M. J.; Trucks, G. W.; Schlegel, H. B.; Scuseria, G. E.; Robb, M. A.; Cheeseman, J. R.; Scalmani, G.; Barone, V.; Petersson,

G. A.; Nakatsuji, H.; Li, X.; Caricato, M.; Marenich, A. V.; Bloino, J.; Janesko, B. G.; Gomperts, R.; Mennucci, B.; Hratchian, H. P.; Ortiz, J. V.; Izmaylov, A. F.; Sonnenberg, J. L.; Williams; Ding, F.; Lipparini, F.; Egidi, F.; Goings, J.; Peng, B.; Petrone, A.; Henderson, T.; Ranasinghe, D.; Zakrzewski, V. G.; Gao, J.; Rega, N.; Zheng, G.; Liang, W.; Hada, M.; Ehara, M.; Toyota, K.; Fukuda, R.; Hasegawa, J.; Ishida, M.; Nakajima, T.; Honda, Y.; Kitao, O.; Nakai, H.; Vreven, T.; Throssell, K.; Montgomery, Jr., J. A.; Peralta, J. E.; Ogliaro, F.; Bearpark, M. J.; Heyd, J. J.; Brothers, E. N.; Kudin, K. N.; Staroverov, V. N.; Keith, T. A.; Kobayashi, R.; Normand, J.; Raghavachari, K.; Rendell, A. P.; Burant, J. C.; Iyengar, S. S.; Tomasi, J.; Cossi, M.; Millam, J. M.; Klene, M.; Adamo, C.; Cammi, R.; Ochterski, J. W.; Martin, R. L.; Morokuma, K.; Farkas, O.; Foresman, J. B.; Fox, D. J. Gaussian Development Version; Gaussian: Wallingford, CT, 2016. (32) Jensen, F. Introduction to Computational Chemistry, 2nd ed.; John Wiley & Sons, Ltd.: Chichester, England, 2007; pp 293-296. (33) Foresman, J. B.; Head-Gordon, M.; Pople, J. A.; Frisch, M. J. Toward a Systematic Molecular Orbital Theory for Excited States. J. Phys. Chem. 1992, 96, 135-149.